VOLUME 72, NUMBER 8

JOC Articles

APRIL 13, 2007

© Copyright 2007 by the American Chemical Society

Supramolecular Photochirogenesis with Biomolecules. Mechanistic Studies on the Enantiodifferentiation for the Photocyclodimerization of 2-Anthracenecarboxylate Mediated by Bovine Serum Albumin

Masaki Nishijima,[†] Tamara C. S. Pace,[‡] Asao Nakamura,[§] Tadashi Mori,[†] Takehiko Wada,[†,||] Cornelia Bohne,*[,‡] and Yoshihisa Inoue*[,†,§]

Department of Applied Chemistry, Osaka University and PRESTO, JST, 2-1 Yamada-oka, Suita 565-0871, Japan, Entropy Control Project, ICORP, JST, 4-6-3 Kamishinden, Toyonaka 560-0085, Japan, and Department of Chemistry, University of Victoria, P.O. Box 3065, Victoria, B.C. V8W 3V6, Canada

bohne@uvic.ca; inoue@chem.eng.osaka-u.ac.jp

Received October 26, 2006

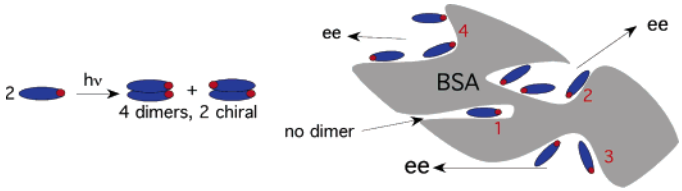

Photophysics and photochemistry of 2-anthracenecarboxylate (AC) bound to bovine serum albumin (BSA) were investigated in detail for the first time by electronic absorption, circular dichroism (CD), steady-state and time-resolved fluorescence, fluorescence quenching, and product analysis studies. Through the spectroscopic investigations, it was revealed that the four independent binding pockets of BSA, which are known to accommodate 1, 3, 2, and 3 AC molecules in the order of decreasing affinity, are distinctly different in hydrophobicity, chiral environment, and accessibility. Interestingly, AC bound to site 1 gave highly structured fluorescence with dual lifetimes of 4.8 and 2.1 ns in an intensity ratio of 3:2, which may be assigned to the existence of two positional or orientational isomers within the very hydrophobic site 1. In contrast, the lifetime of AC in site 2 was much longer (13.3 ns), and ACs in sites 3 and 4 have broader fluorescence spectra with lifetimes that were practically indistinguishable from that in bulk water (15.8 ns). Although each of sites 2−4 simultaneously binds multiple AC molecules, no CD exciton coupling or static fluorescence quenching was detected, indicating that ACs bound to each site are not in close proximity to each other. Quenching studies with nitromethane further confirmed the significant difference in accessibility among the binding sites; thus, ACs bound to sites 1 and 2 are highly protected from the attack of the quencher, affording 32 and 10 times smaller rate constants than that for free AC in water. Product studies in the presence and absence of nitromethane more clearly revealed the photochirogenic performance of each binding site. Although the addition of nitromethane did not greatly alter the product distribution, the enantiomeric excesses (ee's) of chiral cycloadducts **2** and **3** were critically manipulated by selectively retarding the photoreaction occurring at the more accessible binding sites. Thus, the highest ee of 38% was obtained for **2** in the presence of 18 mM nitromethane, while the highest ee of 58% was attained for **3** in the absence of nitromethane, both at [AC]/[BSA] = 3.6.

Introduction

Asymmetric photochemistry is an alternate method to achieve chirogenesis compared to thermal catalytic and enzymatic asymmetric syntheses, and photochirogenesis could find application in chemistry, pharmacology, medical sciences, and agriculture.[1−3] One strategy in asymmetric photochemistry is

[†] Osaka University.
[‡] University of Victoria.
[§] ICORP, JST.
[||] PRESTO, JST.

(1) Inoue, Y. *Chem. Rev.* **1992**, *92*, 741−770.
(2) *Chiral Photochemistry*; Inoue, Y., Ramamurthy, V., Eds.; Marcel Dekker: New York, 2004.

10.1021/jo062226b CCC: $37.00 © 2007 American Chemical Society
Published on Web 01/20/2007

SCHEME 1. Enantiodifferentiating Photodimerization of 2-Anthracenecarboxylate

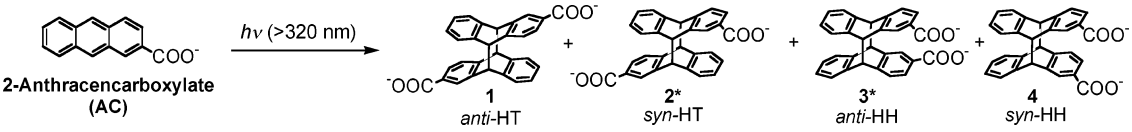

to employ chiral supramolecular environments, such as cyclodextrins,[4−7] zeolites with chiral modifications,[8−10] DNA,[11] hydrogen-bonding templates,[12−14] and chiral crystal lattices.[14−17] The premise for these studies is that weak intermolecular interactions, such as hydrogen bonding, electrostatic interaction, $\pi-\pi$ stacking, hydrophobic interaction, and van der Waals forces, can create a three-dimensional chiral space which influences the outcome of the photochemical reactions, but the building components of the supramolecular system are not incorporated into the product.

Serum albumins are blood carrier proteins, which have several different binding pockets with different binding abilities.[18] These proteins can be viewed as natural chiral host systems. Zandomeneghi et al. used bovine serum albumin (BSA) to study the photodecomposition of 1,1′-binaphthol and ketoprofen.[19−21] Photolysis of racemic compound in the presence of BSA led to the enatiomeric enhancement due to selective binding and preferential excitation of one of the enantiomeric guest pairs. Photophysical studies showed that the triplet lifetimes for the enantiomers of carprofen[22] and flurbiprofen methyl ester[23] in the presence of human serum albumin are different. This difference was suggested to be due to the presence of multiple binding sites with different binding affinities for each enantiomer. These examples showed how proteins can be used as templates for photochirogenesis, but they all involved unimolecular reactions. To broaden the scope of the use of biomolecules for asymmetric photochemistry it is important to establish how these host systems can be used to affect the enantiodifferentiation for bimolecular reactions. The photodimerization of 2-anthracenecarboxylate (AC) was used as a model bimolecular reaction. Photoirradiation of AC leads to the formation of four [4 + 4] regioisomers, i.e., the *anti*- (**1**) and *syn-head-to-tail* (**2**), and *anti*- (**3**) and *syn-head-to-head* (**4**) isomers (Scheme 1). Of the four isomers, **2** and **3** are chiral. This model bimolecular reaction has been previously employed to study the photochirogenesis for AC complexed to cyclodextrins.[24−29]

In a preliminary communication,[30] we reported the binding studies of AC with BSA. From the modeling of the binding isotherms determined from CD, fluorescence and absorption measurements, it was proposed that AC was bound to four sites with individual binding constants of $K_1 = 5.3 \times 10^7\ M^{-1}$, $K_2 = 1.\ 3 \times 10^5\ M^{-1}$, $K_3 = 1.4 \times 10^4\ M^{-1}$, and $K_4 = 3 \times 10^3\ M^{-1}$. The number of ACs bound to each type of site was determined to be 1, 3, 2 and 3 for the sites with decreasing binding affinities.[30] It is important to note that the binding of subsequent ACs to each binding site is treated as independent and it is not known if the ACs with equivalent binding constants all bind to the same region in the protein. Indeed, no exciton coupling was observed in the CD spectra suggesting that the ACs are not in close proximity, even if they are bound to one binding site. This working model will be employed in the current work.

Complexation of AC to BSA affects the ratio of the *head-to-tail* (HT) and *head-to-head* (HH) products formed, where a higher degree of HH products were observed when the AC/BSA ratio was low. In addition, the changes in the enantiomeric excess (ee) for compounds **2** and **3** with the decrease in the AC/BSA ratio were quantitatively different, suggesting that, at least partially, the chiral products were formed in different binding sites of the BSA. This preliminary report also suggested that the enantiodifferentiation was achieved by intra-protein reaction, but an influence from AC free in solution was also relevant.[30]

The complexity of the behavior of the ee with the changes in the BSA concentration suggested that products with opposite chirality might have been formed in the different binding sites of BSA. The objective of the current work was to use photophysical measurements to gain mechanistic information on how BSA leads to the photochirogenesis observed.

(3) Rau, H. *Chem. Rev.* **1983**, *83*, 535−547.
(4) Yang, C.; Inoue, Y. In *Cyclodextrin Materials Photochemistry, Photophysics and Photobiology*; Douhal, A., Ed.; Elsevier: Amsterdam, 2006; Chapter 11.
(5) Inoue, Y.; Dong, F.; Yamamoto, K.; Tong, L.-H.; Tsuneishi, H.; Hakushi, T.; Tai, A. *J. Am. Chem. Soc.* **1995**, *117*, 11033−11034.
(6) Inoue, Y.; Wada, T.; Sugahara, N.; Yamamoto, K.; Kimura, K.; Tong, L.; Gao, X.; Hou, Z.; Liu, Y. *J. Org. Chem.* **2000**, *65*, 8041−8050.
(7) Rao, V. P.; Turro, N. J. *Tetrahedron Lett.* **1989**, *30*, 4641−4644.
(8) Joy, A.; Ramamurthy, V.; Scheffer, J. R.; Corbin, D. R. *Chem. Commun.* **1998**, 1379−1380.
(9) Joy, A.; Scheffer, J. R.; Ramamurthy, V. *Org. Lett.* **2000**, *2*, 119−121.
(10) Wada, T.; Shikimi, M.; Inoue, Y.; Lem, G.; Turro, N. J. *Chem. Commun.* **2001**, 1864−1865.
(11) Wada, T.; Sugahara, N.; Kawano, M.; Inoue, Y. *Chem. Lett.* **2000**, 1174−1175.
(12) Bach, T.; Bergmann, H.; Grosch, B.; Harms, K. *J. Am. Chem. Soc.* **2002**, *124*, 7982−7990.
(13) Cauble, D. F.; Lynch, V.; Krische, M. J. *J. Org. Chem.* **2003**, *68*, 15−21.
(14) Chong, K. C. W.; Sivaguru, J.; Shichi, T.; Yoshimi, Y.; Ramamurthy, V.; Scheffer, J. R. *J. Am. Chem. Soc.* **2002**, *124*, 2858−2859.
(15) Koshima, H. In *Organic Solid-State Reactions*; Toda, F., Ed.; Kluwar Academic Publishers: Dordrecht, The Netherlands, 2002; pp 189−268.
(16) Sakamoto, M.; Sekine, N.; Miyoshi, H.; Mino, T.; Fujita, T. *J. Am. Chem. Soc.* **2000**, *122*, 10210−10211.
(17) Toda, F.; Tanaka, K.; Miyamoto, H. In *Molecular and Supramolecular Photochemistry*; Ramamurthy, V., Schanze, K. S., Eds.; Marcel Dekker: New York, 2001; Vol. 8, pp 385−425.
(18) Peters, T., Jr. *All About Albumin: Biochemistry, Genetics, and Medical Applications*; Academic Press: San Diego, 1996.
(19) Levi-Minzi, N.; Zandomeneghi, M. *J. Am. Chem. Soc.* **1992**, *114*, 9300−9304.
(20) Ouchi, A.; Zandomeneghi, G.; Zandomeneghi, M. *Chirality* **2002**, *14*, 1−11.
(21) Cavazza, M.; Festa, C.; Lenzi, A.; Leviminzi, N.; Veracini, C. A.; Zandomeneghi, M. *Gazz. Chim. Ital.* **1994**, *124*, 525−532.
(22) Lhiaubet-Vallet, V.; Sarabia, Z.; Boscá, F.; Miranda, M. A. *J. Am. Chem. Soc.* **2004**, *126*, 9538−9539.
(23) Jiménez, M. C.; Miranda, M. A.; Vayá, I. *J. Am. Chem. Soc.* **2005**, *127*, 10134−10135.
(24) Nakamura, A.; Inoue, Y. *J. Am. Chem. Soc.* **2003**, *125*, 966−972.
(25) Nakamura, A.; Inoue, Y. *J. Am. Chem. Soc.* **2005**, *127*, 5338−5339.
(26) Tamaki, T.; Kokubu, T. *J. Inclusion Phenom.* **1984**, *2*, 815−822.
(27) Tamaki, T.; Kokubu, T.; Ichimura, K. *Tetrahedron* **1987**, *43*, 1485−1494.
(28) Yang, C.; Fukuhara, G.; Nakamura, A.; Origane, Y.; Fujita, K.; Yuan, D.-Q.; Mori, T.; Wada, T.; Inoue, Y. *J. Photochem. Photobiol. A Chem* **2005**, *173*, 375−383.
(29) Yang, C.; Nakamura, A.; Fukuhara, G.; Origane, Y.; Mori, T.; Wada, T.; Inoue, Y. *J. Org. Chem.* **2006**, *71*, 3126−3136.
(30) Wada, T.; Nishijima, M.; Fujisawa, T.; Sugahara, N.; Mori, T.; Nakamura, A.; Inoue, Y. *J. Am. Chem. Soc.* **2003**, *125*, 7492−7493.

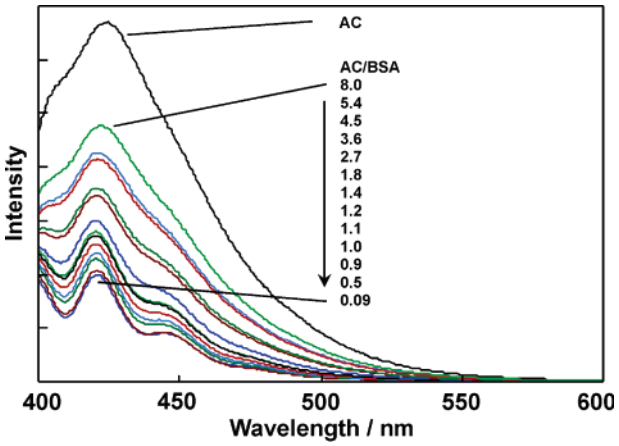

FIGURE 1. Fluorescence emission spectrum of AC (30 μM) in buffer and spectra at various ratios of AC/BSA from 8.0 to 0.09. Absorbancies were matched at the excitation wavelength of 383 nm.

Results

Fluorescence Spectra and Lifetimes. In aqueous buffer solution at pH 7.0 AC was deprotonated, and its emission spectrum was broad. In the presence of BSA the AC fluorescence emission intensity decreased and the spectra sharpened (Figure 1). The spectra at high concentrations of BSA were similar to the spectrum observed for the fluorescence of protonated AC in pentane (see Figure S1 in the Supporting Information). The changes in the width of the AC fluorescence spectra can be compared when the emission spectra at various AC/BSA ratios are normalized (see Figure S2 in the Supporting Information). The same width was observed for AC/BSA ratios equal to or smaller than 0.5, while a slight broadening, which is particularly noticeable between 400 and 450 nm, was observed when this ratio was increased from 0.9 to 1.8. The emission spectrum broadens significantly for AC/BSA ratios above 1.8.

The fluorescence decay of AC in water determined at several wavelengths and two concentrations of AC (1 and 30 μM) was monoexponential, and the lifetime was determined to be 15.8 $\pm$ 0.6 ns (3 determinations). This value is in agreement with the lifetime of 16 ns previously determined.[24] In the presence of BSA, the fluorescence decay did not follow a monoexponential function at any AC/BSA ratio studied. Based on the previous thermodynamic characterization, AC is only bound to site 1 of BSA at AC/BSA ratios equal to and smaller than 0.54. Nevertheless, the emission decay was not adequately fit to a single-exponential decay but nicely fit to the sum of two exponentials and the values for the lifetimes and pre-exponential factors were the same for AC/BSA ratios between 0.027 and 0.54 (see Table S1 in the Supporting Information for individual values). In addition, the same lifetimes and pre-exponential factors were observed when the decay was measured at 420 and 445 nm. The average values for the two lifetimes were 4.8 $\pm$ 0.2 ns and 2.1 $\pm$ 0.2 ns with corresponding pre-exponential factors of 0.58 $\pm$ 0.05 and 0.42 $\pm$ 0.05. In order to compare changes in intensities in the steady-state spectra with changes in lifetimes, average lifetimes corresponding to the integral of the decay curves were calculated using eq 1. The average lifetime for AC at AC/BSA $\leq$ 0.54 was 3.7 $\pm$ 0.3 ns. These shorter lifetimes in the presence of BSA are consistent with the decrease observed for the steady-state emission intensity when AC is bound to the protein. It is important to note that some variability in the lifetimes was observed for different lots of BSA, probably reflecting the heterogeneity of the protein samples, but in all cases the decay did not follow a monoexponential function. This variability underscores the importance of performing the product and photophysical studies with the same lot of BSA, as was done in this study.

$$\langle\tau\rangle = \sum_{1}^{i} A_i\tau_i$$

where

$$\sum_{1}^{i} A_i = 1 \qquad (1)$$

At higher AC/BSA ratios, the AC emission decay was not adequately fit to the sum of two exponentials and a third component was included in the fit, which had a longer lifetime than the two components observed at low AC/BSA ratios. In the presence of all BSA concentrations some AC will be bound to site 1 because of its high equilibrium constant. For this reason, two lifetimes were fixed to the values of 4.8 and 2.1 ns and the third lifetime was recovered from the fit of the fluorescence decay. For an AC/BSA ratio of 0.9 the third lifetime was 13.3 $\pm$ 0.9 ns (3 determinations) with a small pre-exponential factor of 0.02 $\pm$ 0.01. At this ratio, most of the AC is bound to site 1 of the BSA with a small amount (ca. 7%, see Table S2 in the Supporting Information) bound to site 2. This result suggests that the lifetime for AC in site 2 is somewhat shorter than the AC singlet excited-state lifetime in water (15.8 ns). As the AC/BSA ratio was raised the pre-exponential factor for the third component increased from 0.1 at a ratio of 1.8 to 0.6$-$0.7 at a ratio of 8.0 (see Table S3 in the Supporting Information for values at intermediate AC/BSA ratios). In addition, the lifetime for the third component lengthened with the increase of the AC/BSA ratio. The pre-exponential factors for the emission decays collected at 420 and 445 nm were different for AC/BSA ratios equal to or larger than 3.6, suggesting that species with different spectra were present in these solutions. The pre-exponential factors are different from the AC populations calculated from the equilibrium constants (compare Tables S2 and S3), which is unexpected for fluorophores with short lifetimes. This lack of correlation is probably due to the fact that the lifetimes for sites 2, 3, and 4 and in water are slightly different but cannot be deconvoluted in the fluorescence decays.

Relationship of Intensities and Average Lifetimes. The shorter lifetimes for AC in the presence of BSA are consistent with the decrease in the steady-state emission intensity of AC in the presence of the protein. However, the decrease in the steady-state emission intensity could also be related to the static photodimerization of two ACs located in close proximity. For such a static process, the decrease in the steady-state emission intensities would be larger than the shortening of the lifetimes. The dependence of the average lifetimes (see values in Table S4 in the Supporting Information) and the integrated steady-state intensities on the AC/BSA ratio showed a good agreement (Figure 2).

Product Studies in the Presence of Nitromethane. Nitromethane is an efficient quencher of the singlet excited-state of AC (see below). A comparison of the product distribution in the presence and absence of 18 mM nitromethane at various AC/BSA ratios showed that neither the conversion nor the product distribution changed in the presence of nitromethane

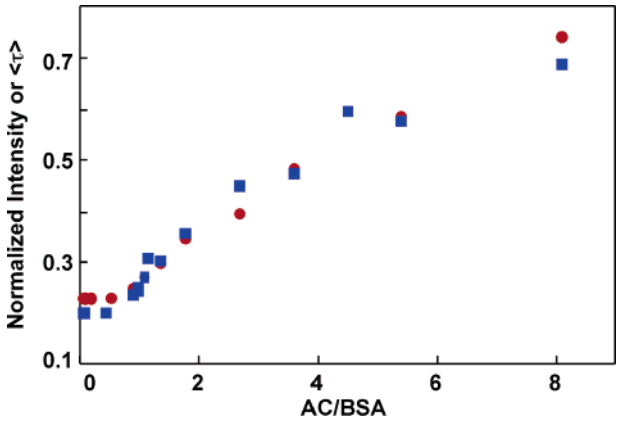

FIGURE 2. Dependence of fluorescence emission intensity (square, blue) and average lifetime (circle, red) on the AC/BSA ratio. Data are normalized to unity for AC in buffer (normalized point not shown).

for an AC/BSA ratio of 3.6, but the ee increased for **2**, while a decrease was observed for **3** (Table 1). At the higher AC/BSA ratios the conversion was smaller, which is consistent with quenching of accessible ACs. The product distribution remained the same for an AC/BSA ratio of 8.0 and 18. A change with the addition of nitromethane was observed for the ee values, with a slight increase in the enantiodifferentiation being observed for **2**, while a large decrease of the ee was observed for **3** at an AC/BSA ratio of 8.0, and the inverse effect, i.e., a large increase, was observed at the higher AC/BSA ratio of 18.

Ground-State Interaction of BSA and Nitromethane. In order to interpret the results of the product studies in the presence of nitromethane it is important to establish if nitromethane binds with BSA or leads to the denaturation of the protein. CD spectra in the presence and absence of nitromethane show minor changes to the protein peaks at 209 and 222 nm, which correspond to the double minimum peaks of the protein α-helix,[18] suggesting that in the presence of 18 mM nitromethane the BSA structure was intact (see Figure S3 in the Supporting Information). The changes at higher nitromethane concentration (74 mM) are probably due to an artifact from the extremely high absorbance of nitromethane at the shorter wavelengths.

The effect of nitromethane (18 mM) on the binding of AC to BSA was investigated further by following the changes in the AC induced circular dichroism signal at 389 nm with the BSA concentration (Figure 3). Up to an AC/BSA ratio of 4.0 the addition of nitromethane did not have an effect on the binding isotherm showing that AC binding to sites 1 and 2 was unaffected by the presence of nitromethane. An increase in the magnitude of the negative induced circular dichroism signal was observed for AC/BSA ratios in the range between 4 and 6, suggesting that nitromethane affects the binding of AC in particular to site 3. The binding efficiency of AC seems to be increased in the presence of nitromethane, which could be a consequence of nitromethane binding to site 3 and increasing its hydrophobicity. Much smaller effects were observed for the binding of AC to site 4.

AC Fluorescence Quenching by Nitromethane. Fluorophores located in different environments but with similar lifetimes can be more easily differentiated when using selective quenchers that interact more efficiently with one species. Nitromethane was used as a quencher for the AC singlet excited state. Quenching can be measured either as a decrease in the emission intensity or as a shortening of the lifetime of the fluorophore. When only dynamic (bimolecular) quenching occurs eq 2 applies, where the Stern−Volmer constant (K_{sv}) corresponds to the product of the quenching rate constant (k_q) and the lifetime of AC in the absence of quencher (τ_o).

$$\frac{I_0}{I} = \frac{\tau_0}{\tau} = 1 + K_{sv}[Q] \qquad (2)$$

For the quenching of aqueous AC by nitromethane, the ratio of lifetimes showed a linear dependence with the quencher concentration leading to a Stern−Volmer constant of 91.6 ± 0.5 M^{-1} and a quenching rate constant of (5.8 ± 0.2) × 10^9 M^{-1} s^{-1}. This value is close to the diffusion-controlled rate constant in water (7.4 × 10^9 M^{-1} s^{-1}).[31] The quenching plot for the change in intensities showed a slight upward curvature indicating that a weak complex (K_{eq} = 4.1 ± 0.8 M^{-1}, see the Supporting Information) was formed between the ground state of AC and nitromethane. The details for the mechanism of complex formation, e.g., C−H···π interactions or nonspecific hydrophobic interactions, were not elucidated and are beyond the scope of this work. However, the possibility of complex formation has to be kept in mind when analyzing the quenching data of AC by nitromethane in the presence of BSA.

For the quenching studies of the BSA bound singlet excited-state of AC with nitromethane it was necessary to use nitromethane concentrations in excess of 20 mM. Based on the control experiments described above, caution has to be employed for the interpretation of the quenching at high nitromethane concentrations. The quenching efficiency of AC by nitromethane decreased as the AC/BSA ratio decreased (Figure 4). A very low quenching efficiency was observed for an AC/BSA ratio of 0.09, suggesting that AC is very well protected from nitromethane quenching when bound to site 1 of BSA. The quenching plot at an AC/BSA ratio of 0.09 was linear even at high nitromethane concentrations. If the quencher denatured the protein one would have expected a release of AC and an upward curvature of the quenching plots. This result is in line with the circular dichroism experiment described above where the binding isotherm for the AC binding to site 1 was not disrupted with the addition of nitromethane.

At AC/BSA ratios larger than 0.09 the quenching plot curved downward, suggesting that different AC species were present, where the species with higher exposure were quenched more efficiently at the lower concentrations of nitromethane. At the higher AC/BSA ratios AC is bound to all four binding sites and some of the curvature could be due to binding of nitromethane to the protein. In this case nitromethane would have to bind at a distance from AC but lead to an alteration of the BSA structure. Nitromethane cannot be bound closely to the ACs because static quenching would occur leading to an upward curvature of the quenching plot, contrary to the experimental observation.

The shape of the fluorescence spectra for AC in aqueous solution and for AC/BSA ratios equal to or smaller than 0.9 did not change with increasing concentrations of nitromethane, whereas for intermediate AC/BSA ratios a sharpening of the emission spectra was observed as the concentration of quencher was raised (see Figure S5 in the Supporting Information for selected AC/BSA ratios). The shape of the emission spectra is

(31) Murov, S. L.; Carmichael, I.; Gordon, L. H. *Handbook of Photochemistry*, 2nd ed.; Marcel Dekker: New York, 1993.

TABLE 1. Effect of Nitromethane Addition on the Photoreaction of AC with BSA[a]

			product distributions[c]/%				% ee[d]		ratio		
[AC]/[BSA]	CH_3NO_2/mM	conversion[b]/%	**1**	**2**	**3**	**4**	**2**	**3**	HH/HT[e]	**1/2**	**3/4**
3.6	0	18	13	14	40	33	−22	58	2.7	0.92	1.2
	18	18	15	15	37	33	−38	48	2.3	1.0	1.1
8.0	0	61	25	23	28	24	−20	50	1.1	1.1	1.2
	18	52	27	21	29	23	−23	34	1.1	1.3	1.3
18	0	67	32	27	23	18	−11	23	0.69	1.2	1.3
	18	62	29	23	28	20	−17	31	0.92	1.3	1.4

[a] Irradiated at >320 nm for 1 h under Ar at 25 °C; [AC] = 0.60 mM. [b] Error ~2%. [c] Error ~2%. [d] Enantiomeric excess determined by chiral HPLC; error <5% ee; the positive/negative ee sign corresponds to the excess of the first/second-eluted enantiomer, respectively. [e] [**3** + **4**]/[**1** + **2**].

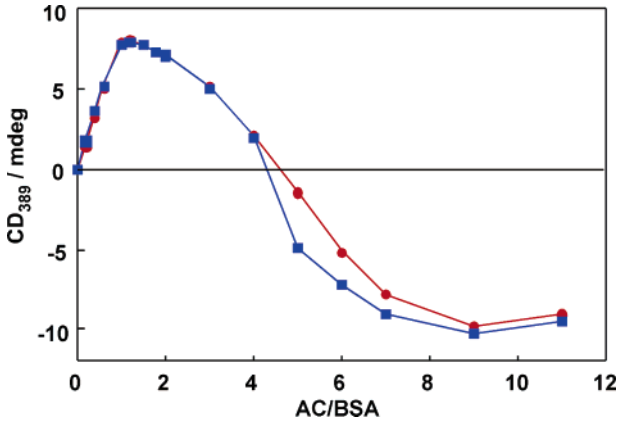

FIGURE 3. Intensity changes for the circular dichroism signal at 389 nm at various AC/BSA ratios in the presence (■) and absence (●) of 18 mM nitromethane at 25 °C. The BSA concentration was kept constant at 0.075 mM, while the AC concentration was varied from 0 to 0.83 mM.

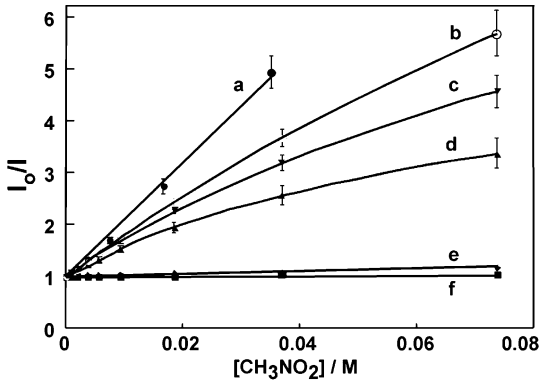

FIGURE 4. Stern−Volmer plot for quenching of AC by nitromethane in the absence (a) and presence of BSA (b, AC/BSA = 8; c, AC/BSA = 3.6; d, AC/BSA = 1.8; e, AC/BSA = 0.9; f, AC/BSA = 0.09).

a composite of the spectra for all AC species, but species with longer lifetimes contribute to a larger fraction of the emission spectrum. The fact that the spectra did not change shape at the low AC/BSA ratios suggests that only one AC species was present. At the high AC/BSA ratios the ACs in water and in the exposed sites of BSA were quenched preferentially and the shape of the spectrum changes from that for AC exposed to water and with a long lifetime to the shape of the spectrum for AC bound to protected sites in the BSA.

The curved quenching plots were fit to eq 3, where F_i is the fraction of the integrated fluorescence spectrum corresponding to species *i*, which has a Stern−Volmer constant of $K_{sv,i}$. Two or three independent quenching experiments were performed and the individual quenching plots were fit to eq 3. Analysis of the quenching plots was performed to estimate the quenching rate constants for AC bound to the various sites of BSA (Table 2). The quenching rate constants indicate the accessibility of nitromethane to the BSA bound AC. The relevant comparison is that for the quenching rate constants and not for the Stern−Volmer constants because the lifetimes of AC in the various sites of BSA were different. Therefore, a more detailed analysis of the K_{sv} values is required.

$$\frac{I_o}{I} = \frac{1}{\sum_1^i \left(\frac{F_i}{1 + K_{sv,i}[Q]} \right)} \qquad (3)$$

For the AC/BSA ratio of 0.09 the quenching plot was linear and the recovered K_{sv} value was much lower (by a factor of over 100) than observed for the quenching in water. The value determined at the AC/BSA ratio of 0.09 was fixed for the quenching plots at higher ratios because there is always a fraction of AC bound to site 1 of the BSA. At the AC/BSA ratio of 0.9 a small amount of AC is bound to site 2 and the fraction bound to sites 3 and 4 and in water is very small. Therefore, the second species observed for this AC/BSA ratio is representative of the quenching of AC in site 2. The K_{sv} value recovered was about 1 order of magnitude larger than for the quenching of AC bound to site 1. The quenching plot for an AC/BSA ratio of 3.6 could not be fit to two components with one of the values fixed for the Stern−Volmer constant for AC bound to site 1. For this reason, a fit considering 3 species was employed, assuming the values for the K_{sv} of AC in sites 1 and 2. The detection of three species at an AC/BSA ratio of 3.6 is consistent with the AC fractions of ca. 0.2, 0.3 and 0.4 in water and bound to sites 1 and 2, respectively. In the case of the higher AC/BSA ratios, the quenching plot curved much less than at the lower ratios and the plots were fit by considering two species where one species was fit either to the K_{sv} value of AC in site 1 or the K_{sv} for AC in site 2. This procedure was followed to obtain information about the K_{sv} values for the less protected sites; i.e., we were interested in establishing if the Stern−Volmer constant for AC bound to sites 3 and 4 could be differentiated from the quenching of AC in water. We also made an attempt to fix the K_{sv} value in water in order to resolve the Stern−Volmer constants for AC in sites 3 and 4 by fitting the quenching plot to three species. However, no additional species could be resolved from this analysis.

Addition of nitromethane to an AC/BSA solution with a ratio of 0.09 did not significantly affect the lifetimes measured up to the highest concentration studied, 35 mM nitromethane. This

TABLE 2. Average Stern−Volmer Constants ($K_{sv,i}$) and Emission Fractions (F_i) Recovered from the Steady-State Quenching Plots at Various AC/BSA Ratios

[AC]/[BSA]	$K_{sv,1}/M^{-1}$	F_1	$K_{sv,2}/M^{-1}$	F_2	$K_{sv,3}/M^{-1}$	F_3
0.09[a]	0.68 ± 0.08	1.00				
0.9	0.68[b]	0.71 ± 0.08	9 ± 4	0.27 ± 0.07		
3.6	0.68[b]	0.07 ± 0.01	9[b]	0.27 ± 0.04	136 ± 24	0.69 ± 0.03
5.4[c]		0.11 − 0.23			91−125	0.80 − 0.90
8.0[c]		0.06 − 0.13			93−110	0.90 − 0.96

[a] Quenching plots were linear. [b] Value fixed. [c] The values quoted are ranges when $K_{sv,1}$ was fixed to either 0.68 or 9 M^{-1}.

TABLE 3. BSA-Mediated Photocyclodimerization of AC in Aqueous Buffer Solutions Containing 0−30% Ethanol[a]

			product distributions[c]/%				% ee[d]		ratio		
[AC]/[BSA]	EtOH /%	conversion /%[b]	**1**	**2**	**3**	**4**	**2**	**3**	HH/HT[e]	**1/2**	**3/4**
9.0	0	54	27	23	28	22	−16	41	1.0	1.2	1.3
	5	59	27	20	30	23	−12	37	1.1	1.4	1.3
	10	58	28	21	29	22	−9	31	1.0	1.3	1.4
	20	53	34	24	25	17	−1	20	0.72	1.5	1.5
	30	59	39	30	19	12	0	7	0.45	1.3	1.6

[a] Irradiated at >320 nm for 1 h under Ar at 25 °C; [AC] = 0.60 mM. [b] Error ∼2%. [c] Error ∼2%. [d] Enantiomeric excess determined by chiral HPLC; error <5% ee; the positive/negative ee sign corresponds to the excess of the first/second-eluted enantiomer, respectively. [e] **([3 + 4])/([1 + 2])**.

result was expected based on the low K_{sv} value determined from the steady-state experiments. Therefore, the upper limit for the quenching rate constant of AC in site 1 calculated from the K_{sv} value of 0.68 M^{-1} and the average lifetime of 3.7 ns is (1.8 ± 0.3) × 10^8 M^{-1} s^{-1}. This value is 32 times lower than for the quenching of AC in water. It is important to note that the decrease in the Stern−Volmer constant for AC bound to site 1 in BSA when compared to the K_{sv} value in water is due to a lower quenching rate constant and due to the reduction of the AC singlet excited-state lifetime.

The emission decay for an AC/BSA ratio of 0.9 was fit to the sum of three exponentials where the first two lifetimes were kept constant to the values observed for lower AC/BSA ratios. The third lifetime decreased slightly with the addition of nitromethane. However, the data were too scattered to be analyzed using a quenching plot. The quenching rate constant for AC bound to site 2 was estimated from the K_{sv} value of the second species determined in the steady-state experiments (9 M^{-1}) and the lifetime of the third component in the absence of quencher (13.3 ns), where the first two components correspond to AC bound to site 1 and are related to the low K_{sv} value discussed above. The value of 7 × 10^8 M^{-1} s^{-1} is approximately 1 order of magnitude smaller than the quenching rate constant in water. The comparison of the quenching rate constants shows that AC in site 1 is significantly more protected than the AC in site 2 of the BSA. No differentiation of AC bound to sites 3 and 4 and the AC free in water was possible from quenching studies at AC/BSA ratios higher than 0.9. This result indicates that the lifetimes and quenching efficiencies for the ACs in sites 3, 4 and in water are very similar.

The ratio of intensities and lifetimes for the steady-state and time-resolved quenching experiments were compared at several AC/BSA ratios. At the low AC/BSA ratios (≤0.9) the values for I_o/I and τ_o/τ were very similar, but the difference increased as the AC/BSA ratio was raised (Table S5 in the Supporting Information). However the difference between the two ratios was always the same or lower than the difference observed for AC quenching by nitromethane in aqueous solution. This result suggests that AC binding to BSA suppressed the formation of the complex between AC and nitromethane; this complex, which would lead to static quenching, was not formed within the protein.

Effect of Ethanol Addition to the Photodimerization of AC. Experiments were performed in water/ethanol mixtures to establish the effect of protein denaturation on the product distribution for the photodimerization of AC in the presence of BSA. First, we examined the CD spectra of BSA in aqueous buffer solutions containing 0−30% ethanol as cosolvent, but no appreciable change was observed under the conditions employed, suggesting that there is no significant denaturation or conformational change in BSA. Photochemically, the addition of ethanol did not affect the conversion of AC and up to 10% cosolvent did not alter the HH/HT ratio (Table 3). However, the ee for **2** and **3** were decreased in both cases. At the higher ethanol concentrations of 20−30%, the HH/HT ratio changed, and no ee was observed for **2**, while for **3** the ee decreased significantly.

Discussion

The objective of this work was to use a combination of photophysical characterization and product studies in the presence of quenchers to gain mechanistic insights on the photochirogenic dimerization of AC induced by BSA. AC was previously proposed to bind to 4 different sites in BSA, where the binding stoichiometries were determined to be 1, 3, 2, and 3 for sites 1−4; site 1 being the one with highest affinity and site 4 the one with lowest affinity.[30]

The singlet excited-state lifetimes for AC bound to all sites of BSA were equal to or shorter than 16 ns. The equilibrium constant for each site is equal to the ratio of the association rate constant of AC in water with the BSA and the dissociation rate constant of AC from BSA into the aqueous phase ($K = k_+/k_-$). The highest value for k_+ is the value for a diffusion-controlled process (7 × 10^9 M^{-1} s^{-1}). Assuming that the equilibrium constants for ground and excited state AC are similar, and based on the equilibrium constants previously determined,[30] the shortest residence time of AC ($1/k_-$) is calculated to be 8 ms for site 1 to 430 ns for site 4. These residence times are much longer than the singlet excited-state lifetimes for AC and, therefore, the excited-state of AC does not exit from any of the sites in the BSA to the aqueous phase during its lifetime. The concentrations of BSA are too low (≤ 1.0 mM) for association of any singlet excited AC in water

with the protein to occur before the excited-state decays back to the ground state. These calculations are based on the equilibrium constants defined for concentrations of AC bound to BSA and AC free in water and for this reason no conclusions can be reached about the intra-protein mobility of the excited-state of AC. It is important to note that the mobility of ground state AC is not restricted by a finite lifetime, as is the case for the excited state. For this reason product formation can occur due to the mobility of ground state AC between the aqueous phase and BSA and also due to mobility of ground state AC molecules within the protein matrix.

The fluorescence spectrum of AC bound to site 1 shows the vibrational structure observed for the emission of protonated AC in nonpolar solvents. This result indicates that AC is bound to a nonpolar environment and could possibly be hydrogen bonded to an amino acid residue. The lifetime of AC in site 1 was much shorter than in water suggesting that AC is located close to amino acids that can quench its excited state, such as tryptophans or tyrosines; indeed, BSA contains 2 Trp and 19 Tyr residues. The two lifetimes are an intrinsic feature of the binding of AC to site 1 because the ratios of the pre-exponential factors did not change with decreasing AC/BSA ratios. The presence of the two lifetimes could be either due to protein heterogeneity or due to changes in the relative alignment of AC in the binding site.

The singlet excited-state of AC bound to site 1 is very well protected from the interaction with nitromethane, where the quenching rate constant was determined to be lower than 2×10^8 M^{-1} s^{-1}. In the presence of the 18 mM nitromethane concentration employed for the product studies less than 1.5% of the excited states of AC in site 1 of BSA are quenched. This result is in line with the sharpening of the fluorescence spectra with the addition of nitromethane at high AC/BSA ratios since only the ACs in sites 2, 3 and 4 are quenched and most of the remaining emission is from AC in site 1. No photoconversion of AC was observed at low AC/BSA ratios suggesting that AC molecules bound to site 1 do not contribute to the formation of products and therefore also do not contribute to the photochirogenesis observed.

AC bound to site 2 has a broader spectrum than observed for AC in site 1. The exact shape of the spectrum cannot be deconvoluted because the contribution of AC in site 2 is always small compared to the proportion of AC in site 1 at intermediate AC/BSA ratios (1−2, see the Supporting Information for the distribution of the AC population). The singlet excited-state lifetime for AC in site 2 (13.3 ns) is only slightly shorter than for AC in water showing that a small environmental effect operates. The quenching of AC in this site by nitromethane is more efficient than for AC in site 1, but is 1 order of magnitude smaller than the quenching rate constant for AC in the aqueous phase. At a concentration of 18 mM, nitromethane quenches 14% of the excited ACs bound to site 2.

AC molecules bound to sites 3 and 4 have fluorescence spectra that are very similar to the spectrum measured for this fluorophore in water. The lifetime for AC in sites 3 and 4 was longer than measured for AC in site 2, and can be assumed to be equal to the AC singlet excited-state lifetime in water. The AC molecules in sites 3 and 4 are quenched with a similar efficiency as observed for the quenching reaction in water. Small changes could be present but our steady-state and time-resolved experiments do not have the resolution for such small differences, even if they are present. Assuming a K_{sv} value of 92 M^{-1}, determined from the lifetime measurements for AC in water, the amount of excited AC quenched in sites 3, 4 and water was 63% of the total number of excited states at a nitromethane concentration of 18 mM.

The average lifetime of a fluorophore is directly proportional to the fluorescence intensity measured in the steady-state experiment. Therefore, when normalizing the intensity and average lifetime data in water and comparing the relative values at increasing BSA concentrations, one can determine if the shortening of the lifetime is the only parameter responsible for the lower AC emission intensities observed. The same dependence was observed for the emission intensities and the average lifetimes, indicating that no static quenching occurred. The latter type of reaction would not have changed the lifetime of AC, since static quenching occurs within the excitation pulse. This result shows that AC molecules in BSA are not located closely enough to undergo static quenching and photodimerization as was the case with the AC−γ-cyclodextrin complex.[24,25] This is an important point because it indicates that *photochirogenesis is not due to binding of two AC molecules to a very selective site from the stereochemical point of view, but involves dynamic processes including either AC molecules in the aqueous phase or mobile AC molecules within the protein.*

Product studies were performed at nitromethane concentrations of 18 mM because this concentration was low enough to avoid the photolysis of nitromethane.[32] Photolysis of nitromethane was possible in the product studies because the irradiation wavelengths were longer than 320 nm and the nitromethane absorption tails out to 350−360 nm. Photolysis is not likely for the fluorescence experiments because the excitation wavelength used was 383 nm.

Aqueous/ethanol solutions were employed to determine the effect of the polarity of the bulk solvent on the photochirogenesis observed. The experiment was performed at a high AC/BSA ratio to ensure that all binding sites of BSA were populated. The values for the product distribution, ee, and HH/HT ratios in the absence of ethanol are the same within experimental errors to those reported earlier.[30] The effect of ethanol is modest up to a concentration of 10%, but at higher concentrations the solvent becomes hydrophobic enough to extract ACs from the BSA binding sites, the product distribution changes significantly and the ee for **2** disappears, while some ee is still present for **3**. This result shows that in the case of **2** all the ee is due to binding of AC to weaker binding sites, while in the case of **3** a small portion of ee can be achieved from the stronger binding sites even in the less hydrophilic solvents. Compound **3** has a HH stereochemistry and the small ee observed at high ethanol concentrations could be due to the alignment of AC in the BSA sites because of electrostatic interactions between AC and positively charged amino acids.

Based on the experiments discussed above, and the preliminary results published earlier,[30] the following conclusions can be reached: (i) AC in site 1 is unreactive and will not contribute to the product distribution in the photodimerization experiments, (ii) no static quenching occurs between singlet excited AC and ground state AC, precluding the formation of dimers from two AC molecules bound in close proximity to one binding site, (iii) no significant static quenching occurs between AC and nitromethane in the BSA. In addition, in the presence of 18 mM nitromethane AC in site 2 is quenched by 14% while ACs

(32) Morrison, H. A. In *The Chemistry of the Nitro and Nitroso Groups, Part 1*; Feuer, H., Ed.; Wiley: New York, 1969; pp 165−213.

TABLE 4. Estimated Populations of AC, Free and Bound to Each Site in BSA, Calculated from the Binding Constants Determined in the Previous Study[a]

	% site population of AC[b] (*number of AC molecules per site*)				
[AC]/[BSA]	site 1	site 2	site 3	site 4	free AC
3.6	27.7 (*1.0*)	55.9 (*2.0*)	10.0 (*0.4*)	3.7 (*0.1*)	2.6 (*0.1*)
8.0	12.5 (*1.0*)	35.6 (*2.8*)	16.7 (*1.3*)	11.3 (*0.9*)	23.9 (*1.9*)
18	5.6 (*1.0*)	16.3 (*2.9*)	9.3 (*1.7*)	8.7 (*1.6*)	60.2 (*10.8*)

[a] Reference 30. [b] [AC] = 0.6 mM.

in sites 3, 4 and water are quenched by 63%. Therefore, in the presence of nitromethane the products formed from the accessible sites 3 and 4 are decreased to a greater extent than the products formed from site 2. The calculated AC population and number of AC molecules per site for the AC concentration used in the photoirradiation experiments (Table 4) are relevant for the analysis of the results.

It is important to note that ACs in site 1 and in water do not contribute to the ee observed. For an AC/BSA ratio of 3.6, site 2 has a higher population of AC than sites 3 and 4 combined and only a very small amount of AC is in water. Therefore, the contribution of the product distribution from reactions in water is minimized under these conditions. It is also important to note that site 2 has, on average, an occupation of 2 ACs. As shown in Table 1, the HH/HT ratio is much higher than the ratio observed in water (0.28),[30] suggesting that alignment of the ACs due to electrostatic interactions is an important component in the chemistry for the product distribution. This means that electrostatic interactions direct the orientation of the AC molecule when it approaches an excited AC before the dimer is formed. In the presence of nitromethane the product distribution and the anti/syn and HH/HT ratios were not significantly altered (Table 1), suggesting that the anti/syn and HH/HT ratios for product formation in sites 2 and 3 are not very different. If this ratio was significantly different in the two sites the contribution to the ratio from site 3 would be less prominent in the presence of the quencher and a trend in the HH/HT values would have been observed.

In the presence of 18 mM nitromethane at an AC/BSA ratio of 3.6, the absolute value of ee for **2** increases from −22% to −38%, while the ee for **3** decreases from 58% to 48% (Table 1). Due to the easier access to site 3 (plus 4) than to site 2, more ACs in site 3 (plus 4) are quenched by nitromethane. In the case of **3** the ee becomes smaller in the presence of nitromethane, indicating that ACs bound to site 3 produce **3** in an ee much better than that obtained in site 2. This result prompted us to estimate hypothetical ee values inherent to sites 2 and 3, although we do not know the difference in AC reactivity in each site. In the following calculations, we assume as the first approximation that: (1) the photodimerization of ACs populating site 4 and bulk solution can be neglected (because of the low population: < 5%) and (2) the photodimerization efficiency is the same for sites 2 and 3. The second assumption is only tentative, since site 2 provides a stronger, better protected binding site than site 3, and therefore the photodimerization of AC should be slower in site 2 (where external attack does not appear to be a dominant path to the photodimer, judging from the high HH/HT ratios at AC/BSA = 3.6). These assumptions allow us to calculate the inherent ee's of **2** and **3** produced in sites 2 and 3. As revealed in the quenching study mentioned above, 18 mM nitromethane quenches the excited ACs in sites 2 and 3 by 14% and 63%, respectively. Since only the ACs not quenched by nitromethane can afford the dimer, the net contributions from sites 2 and 3 are calculated to be 48.1% and 3.7% of total excited AC, respectively, as a product of the population (55.9% and 10%) and the survival factor (0.86 and 0.37) at each site. Thus, in the case of **3** the 48% ee obtained in the presence of nitromethane is a weighted sum of the ee's from sites 2 and 3. Assuming the inherent ee's for sites 2 and 3 as x (%) and y (%), respectively, we obtain eq 4:

$$(48.1x + 3.7y)/51.8 = 48 \quad (4)$$

Similarly, the 58% ee obtained in the absence of the quencher is a weighted sum of the ee's from site 2 (55.9% population) and site 3 (10% population):

$$(55.9x + 10y)/65.9 = 58 \quad (5)$$

From eqs 4 and 5, we obtain the inherent ee's of dimer **3**, which are 39% for site 2 and 164% for site 3 (see the Supporting Information for the details of the calculation), the latter of which is obviously unacceptable. A similar calculation for **2** led to ee values of −52% in site 2 and 148% in site 3. Even if site 4 is included in the calculation (see Supporting Information) ee values above 100% were calculated. This result indicates that assumption (2) fails and the photodimerization in site 2 is appreciably slower or less efficient than that in site 3. If we assume that the reactivity at site 2 is three times slower than in site 3, the ee's for **2** in sites 2 and 3 are respectively −57% and 43%, while the ee's for **3** are 36% (site 2) and 99% (site 3). In addition, values below 100% were obtained if a further decrease in the efficiency was assumed for the reactivity of AC in site 2. This result suggests that the reactivity in site 2 is at least 3 times slower than in site 3. The general trends observed from these calculations are that the ee for **2** in site 3 is positive while in site 2 it is negative, while for product **3** the ee's in both sites are positive and are always higher in site 3 than in site 2.

At an AC/BSA ratio of 8, the populations of AC in site 2 (36%) and in sites 3 + 4 (28%) are similar. It is important to note that the population of AC in water is of the same order of magnitude (24%) and the average occupancy of site 2 is close to 3, while at the lower AC/BSA ratio it was 2. The contribution of dimers formed in water seems to be small because the HH/HT ratio did not change when nitromethane was added to the solution. Quenching of product formation in the aqueous phase should have increased the HH/HT ratio. The different product distributions for the AC/BSA ratios of 3.6 and 8 are therefore a reflection of the different populations of AC in each site. The trends for the ee values in the presence and absence of quencher are the same at an AC/BSA ratio of 8 as those observed for the lower ratio of 3.6, suggesting that the absolute configurations of the products formed in each site did not change. In the absence of the quencher, the ee's for **2** (−20%) and **3** (50%) obtained at AC/BSA = 8 are comparable to or somewhat smaller than those (−22% and 58%, respectively) at AC/BSA = 3.6. In contrast, in the presence of 18 mM nitromethane, the ee's of **2** (−23%) and **3** (34%) at AC/BSA = 8 are much smaller than those (−38% and 48%, respectively) at AC/BSA = 3.6. This result may be rationalized if the product's ee varies with the occupancy of site 2. When AC/BSA = 3.6, site 2 is occupied by two AC molecules and only one mode/pathway of photodimerization is allowed for the two ACs, while at AC/BSA = 8, site 2 contains 3 ACs, each of which can choose one of the

remaining two ACs accommodated in the same site, but the stereochemical consequence of the choice would lead to different ee values.

At the highest AC/BSA ratio employed the population of AC in site 2 (16%) is again similar to the population in sites 3 + 4 (18%), while the population of AC in water is much higher (60%). The contribution from dimers formed in the aqueous phase is now apparent as an increase of the HH/HT ratio in the presence of nitromethane. Although the ee's for both **2** (−11%) and **3** (23%) are much smaller than those (−22 to −20% and 58 to 50%, respectively) obtained at lower AC/BSA ratios, the addition of the quencher increases the ee's for **2** and **3** up to −17% and 31%, respectively. This means that we can minimize the undesirable contribution from the racemic photodimerization in the bulk solution by adding the quencher and consequently enhancing the contribution from the enantiomeric dimers produced in BSA sites, eventually raising the ee value.

Conclusion

In this work, the photochirogenic mechanism for AC accommodated in BSA binding sites was investigated by characterizing each binding site as to its hydrophobicity, accessibility, reactivity and photochirogenic ability. The results obtained from the spectroscopic studies are directly correlated to the photochirogenic behavior of AC molecules accommodated in each BSA binding site. It should be noted that the use of nitromethane as a site-selective quencher not only simplifies the overlapped spectroscopic property/behavior but also serves as a convenient tool for manipulating, and often improving, the stereochemical outcomes of photochirogenic reactions. The largest photochirogenesis was observed for the site with moderate binding affinity (site 3) showing that compensation between the strength of the binding and mobility is important to achieve chiral discrimination for bimolecular reactions in chiral environments. The strategies and methodologies developed in this study are applicable in general to a wide range of supramolecular photochirogenic reactions conducted in rather complicated biomolecules and therefore further encourage the use of chiral binding sites of various biomolecules as attractive photochirogenesis media.

Acknowledgment. The work at the University of Victoria was supported by the Natural Science and Engineering Research Council of Canada (NSERC). M.N. thanks the 21st Century COE Program for Integrated EcoChemistry, Osaka University, and the Yoshida Scholarship Foundation for financial support. T.W. is grateful for the generous support of this work by a Grant-in-Aid for Scientific Research from the Ministry of Education, Science, Sports, and Culture. T.C.S.P. thanks NSERC for a Canadian Graduate Scholarship and the University of Victoria for a Graduate Scholarship.

Supporting Information Available: Experimental details, comparison of the fluorescence spectra for protonated and deprotonated AC, normalized fluorescence spectra at various AC/BSA ratios, AC singlet excited-state lifetimes at various AC/BSA ratios, population of AC at various AC/BSA ratios, average AC lifetimes, circular dichroism spectra for BSA in the presence of nitromethane, details on quenching studies, and calculation of ee's for products **2** and **3**. This material is available free of charge via the Internet at http://pubs.acs.org.

JO062226B